

Contrastive Disentanglement in Generative Adversarial Networks

Lili Pan^{*}, Peijun Tang^{*}, Zhiyong Chen^{*}, Zenglin Xu^{†‡}

Abstract

Disentanglement is defined as the problem of learning a representation that can separate the distinct, informative factors of variations of data. Learning such a representation may be critical for developing explainable and human-controllable Deep Generative Models (DGMs) in artificial intelligence. However, disentanglement in GANs is not a trivial task, as the absence of sample likelihood and posterior inference for latent variables seems to prohibit the forward step. Inspired by contrastive learning (CL), this paper, from a new perspective, proposes contrastive disentanglement in generative adversarial networks (CD-GAN). It aims at disentangling the factors of inter-class variation of visual data through contrasting image features, since the same factor values produce images in the same class. More importantly, we probe a novel way to make use of limited amount of supervision to the largest extent, to promote inter-class disentanglement performance. Extensive experimental results on many well-known datasets demonstrate the efficacy of CD-GAN for disentangling inter-class variation.

1. Introduction

Efforts to understand deep generative models, *e.g.* generative adversarial networks [2, 11, 12, 33, 35, 37, 39], and variational autoencoders [21, 22, 43], have never stopped in recent years—motivated by the ultimate goal of interpretable and human-controllable artificial intelligence [8, 26, 38, 47]. The two main lines are: representation understanding (*e.g.*, disentangling representation [10, 29, 31, 41], seeking the correlation between objects and representations [4]) and model understanding [1, 18, 23, 25, 46, 47, 48].

Learning interpretable representation, means to learn a disentangled representation which can separate the distinct, informative factors of variation in the data. Disentanglement related literature is filled with Bayesian generative models, such as VAE [22], β -VAE [17], and factor-VAE [20], where the representation can be learned through latent variable

models with some structure prior. In contrast, the work about disentanglement in GANs is very rare, even GANs have remarkable ability of generation. Such a contrast forces us to think the reasons behind it, and we think the absence of sample likelihood and posterior inference in GANs seems to prohibit the forward step. Then, a natural question arises, without a probabilistic framework in GANs, how to learn a factorized representation, especially disentangling the inter-class variation.

InfoGAN [7], as one of the few choice for disentanglement methods in GANs, attempts to control the underlying factors by maximizing the mutual information (MI) [3] between the images and latent variables. However, it has three obvious drawbacks: (i) computing the mutual information between factor and image appears not so reasonable, as they lie in different domains; (ii) the optimization of InfoGAN is relatively complex and leads training instability; (iii) it does not provide a way on how to utilize limited amount of supervision, as Locatello *et al.* [30] recently have demonstrated that unsupervised disentanglement learning without inductive biases is theoretically impossible.

Following this line of thinking, we attempt to explore other ways that can address this issue. Inspired by the definition of disentanglement, we have an intuition that the recent successful contrastive learning (CL) [42, 5, 14, 44, 19, 19] may open a door for us—the factor with the same value produce images with similar features and vice versa.

Motivated by this intuition, we propose a new disentanglement framework, namely contrastive disentanglement in generative adversarial networks (CD-GANs), which explore a new way for inter-class disentanglement, and provide possibility to utilize limited amount of supervision to the largest extent. Specifically, we formulate a contrastive loss on class related features to guide the generated images to correlate to latent factors and analyze how such a loss potentially helps GANs training. In addition, we provide a new way to make use of few labels to largest extent for improving inter-class disentanglement performance.

We demonstrate the efficacy of our CD-GAN on a number of well-known datasets: (i) MNIST [27], (ii) Fashion-MNIST [45], (iii) CIFAR-10 [24], (iv) dSprites [32] and (v) Faces [36]. The extensive qualitative and quantitative results demonstrate the inter-class disentanglement capability of our method. Importantly, the results with few labels in our

^{*}University of Electronic Science and Technology of China, Chengdu, China.

[†]Harbin Institute of Technology, Shenzhen, China.

[‡]Peng Cheng Lab, Shenzhen, China.

E-mail addresses: panlili8255@gmail.com

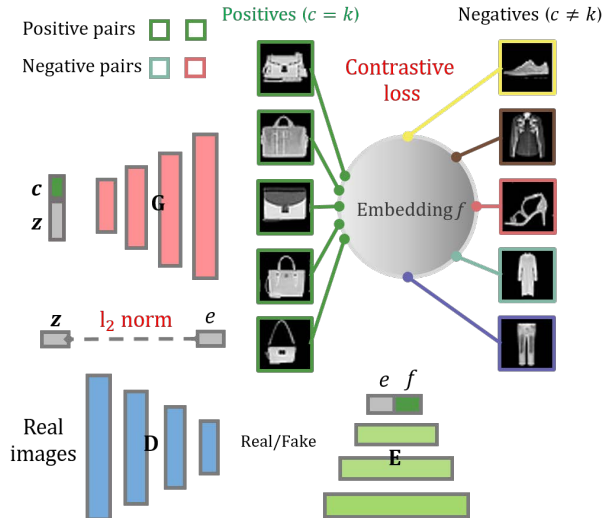


Figure 1. The Network architecture of CD-GAN, which has one generator, one discriminator and one encoder. The input of Generator consists of two parts, one is the continuous latent code z , which represents the content code, the other is one-hot latent factor c , which controls the category of generated images. The discriminator is used to determine whether an image is real or fake, while the encoder is constrained by contrastive loss and l_2 loss. The definitions of positives and negatives are images with the same class or not.

framework can promote the disentanglement performance dramatically.

In summary, in this paper, we make the following contributions: (i) we propose a new inter-class disentanglement framework in GANs, which has the state-of-the-art unsupervised disentanglement performance. (ii) we analyze the advantage of contrastive loss for preventing mode collapse in GANs training. (iii) we probe a new way, in complex data disentanglement, to make use of limited amount of supervision to the largest extent, rendering obvious performance improvement. (iv) we demonstrate the efficacy of our CD-GAN on many well-known tasks and public datasets.

2. Related Works

This section reviews disentanglement in VAE and GANs, and contrastive learning.

Disentanglement in VAE. VAE-based methods [6, 17, 20] attempt to optimize the total correlation (TC) objective, which encourages the independence between each dimension of latent representation. β -VAE [17] uses a larger weight on the KL divergence between the variational posterior and the prior. β -TCVAE [6] estimates TC by minibatch-weighted sampling. Factor-VAE [20] utilizes a discriminator network to estimate the TC. Recently, the work [31] has proposed to use few labels in disentangling factors of variation under the VAE framework. These methods have been shown to be capable of disentangling factors with a successful disentan-

glement scores. However, VAE-based methods has a limited capability of image generation caused by its l_2 norm loss.

Disentanglement in GANs. Disentanglement methods in GANs [9, 7, 28, 34, 40] can be categorized into two types: unsupervised and supervised. InfoGAN [7], as one typical unsupervised method, attempts to control the underlying factors by maximizing the mutual information (MI) between the images and latent vectors. InfoGAN-CR [28] adds a contrastive regularizer over the latent codes. While ClusterGAN [34] sample the one-hot latent vector and the continuous code with a reconstruct loss and a cross-entropy loss to achieve clustering in the latent space. In the direction of supervised disentanglement, Esser *et al.* [9] proposed an invertible interpretation network to disentangled the representations of semantic concepts from hidden representations.

Recently, Locatello *et al.* [30] has demonstrated that unsupervised disentanglement learning without inductive biases is theoretically impossible and that existing inductive biases and *unsupervised methods do not allow to consistently learn disentangled representations*. On the other hand, some work [31] have pointed out that obtaining a limited amount of supervision, for example labelling extremely small number of samples, like 1%, is effective in VAE based methods. However, to the best of our knowledge, there is no related works on how to improve the disentanglement performance by virtue of little supervision in GANs.

Contrastive Learning. As a typical self-supervised representation learning, contrastive learning [42, 5, 14, 44, 19, 19] aims to maximize the characteristic similarity of positive pairs and to minimize it between negative pairs, then the learned representation can be applied to downstream tasks. Contrastive loss is inspired by noise contrastive estimation [13] or N-pair losses [42], and it usually adopts cross-entropy loss, l_2 loss and cosine similarity loss.

Contrastive learning needs to construct positive and negative pairs for training. SimCLR *et al.* [5] introduces data augmentations such as rotation and cutout, and knowledge distillation to construct the single positive pair for every sample, and other images are regarded as negative samples for that sample. Momentum Contrast (Moco) [14, 44] further demonstrates the effect of increasing the number of negative pairs on promoting the performance of contrastive learning. On the contrast, supervised contrastive learning (SCL) [19] uses image-level class labels as the basis for constructing positive and negative pairs, and show appropriately increasing the number of positive samples contributes to improve the performance of CL. Our work is mainly inspired by SimCLR [5] and SCL [19], we introduce contrastive loss into GANs in the hope that it can guide GANs to fulfill inter-class disentanglement.

3. Contrastive Disentanglement in Generative Adversarial Networks

Generative adversarial networks (GANs), as the fundamental deep generative model, directly learn a mapping (*i.e.* generator G) from input noise \mathbf{z} to image, where discriminator D is trained to discriminate real and fake images. Specifically, it trains D to maximize the probability of giving correct discrimination to both real and generative samples, and simultaneously train G to maximize the probability of generated samples being real. The objective function usually takes the form:

$$\min_G \max_D \mathbb{E}_{\mathbf{x} \sim p_{data}(\mathbf{x})} [\log D(\mathbf{x})] + \mathbb{E}_{\mathbf{z} \sim p(\mathbf{z})} [\log (1 - D(G(\mathbf{z})))] . \quad (1)$$

Here, $D(\mathbf{x})$ can be viewed as the probability of \mathbf{x} being real, and $D(G(\mathbf{z}))$ is defined for the generated sample $G(\mathbf{z})$.

As previously mentioned, disentanglement in GANs is not a trivial task, as latent variable model with data structure prior is hard to formulate in the scenario where no sample likelihood exists. Towards breaking through this obstacle, we propose to disentangle the inter-class variation of data through comparing the features of generated images. It is inspired by the intuition the same factor values render the same image feature related to that factor.

To disentangle the inter-class variation of data, which is the commonest in visual data, we define the input latent code consists of two parts: (i) $c \sim \text{mul}(\boldsymbol{\pi})$, which controls the detailed class and (ii) $\mathbf{z} \sim \mathcal{N}(\mathbf{0}, \sigma^2 \mathbf{I})$, which corresponds to intra-class variation. Then, for each generated image $G(\mathbf{z}, c)$, given the discriminator D , the loss for generator now change to be:

$$\mathcal{L}_{GAN} = \mathbb{E}_{\mathbf{z}, c \sim p(\mathbf{z}, c)} [\log (1 - D(G(\mathbf{z}, c)))] . \quad (2)$$

where $p(\mathbf{z}, c)$ can be rewritten as $p(\mathbf{z})p(c)$ as \mathbf{z} and c are independent variables.

Inspired by the intuition that the class factor with the same values should produce images in the same class, we use an encoder to extract its class related representation \mathbf{f} , *i.e.*, $\mathbf{f} = E_f(G(\mathbf{z}, c))$ and construct contrastive loss \mathcal{L}_c with respect to feature \mathbf{f} . We hope the same factor c with the same values, even match with various \mathbf{z} , renders similar features \mathbf{f} , and vice versa. Let $p_{pos}(\cdot, \cdot)$ be the positive distribution about \mathbf{z}, c over $\mathbb{R}^{D+1} \times \mathbb{R}^{D+1}$, $p(\mathbf{z}, \text{neg}(c))$ the distribution of negative samples, *i.e.*, with different class factor value. By virtue of contrasting positive and negative pairs, we formulate \mathcal{L}_c as:

$$\mathbb{E}_{\substack{(\mathbf{z}, c, \mathbf{z}^+, c^+) \sim p_{pos} \\ (\mathbf{z}_i, c_i^-) \stackrel{i.i.d.}{\sim} p(\mathbf{z}, \text{neg}(c))}} \left[-\log \frac{e^{(\mathbf{f}^T \mathbf{f}^+ / \tau)}}{e^{(\mathbf{f}^T \mathbf{f}^+ / \tau)} + \sum_i e^{(\mathbf{f}^T \mathbf{f}_i^- / \tau)}} \right] \quad (3)$$

where $\tau > 0$ is a scalar temperature hyperparameter. Here, \mathbf{f}^+ is the feature learned from positive sample, *i.e.*, $E_f(G(\mathbf{z}^+, c^+))$, $c^+ = c$, \mathbf{z}^+ is a sampling point from $p(\mathbf{z})$ and $\mathbf{z} \neq \mathbf{z}^+$. Similarly, \mathbf{f}_i^- is the feature learned from negative samples, *i.e.*, $E_f(G(\mathbf{z}_i^-, c_i^-))$ and $c_i^- \neq c$. Eq. 3 encourages the generated samples with the same latent code c have similar features \mathbf{f} , and the samples with distinct latent code c have unlike \mathbf{f} , as shown in Fig. 1. Through such a contrastive loss, we can formulate the correlation between the class of generative images and latent code c .

Importantly, suppose the encoder, namely E_f , is ideal, $\mathbb{P}[\mathbf{f} = \mathbf{f}^+] = 1$, the loss \mathcal{L}_c changes to be:

$$\mathbb{E}_{\substack{(\mathbf{z}, c) \sim p(\mathbf{z}, c) \\ (\mathbf{z}_i, c_i^-) \stackrel{i.i.d.}{\sim} p(\mathbf{z}, \text{neg}(c))}} \left[\log \left(e^{1/\tau} + \sum_i e^{(\mathbf{f}^T \mathbf{f}_i^- / \tau)} \right) \right] \quad (4)$$

which is equivalent to maximizing the pairwise distance between \mathbf{f} and \mathbf{f}_i^- in the learned space \mathcal{F} , means pushing the images with different factor values (*e.g.* category) uniformly distributed. This may alleviate the possibility of mode collapse in GANs training.

Except enforcing the class related features to be as similar as possible when factor c has the same value, we also enforce the content not to change with class c to guarantee the c and \mathbf{z} are distinct factors [34]. Even we impose independent assumption on \mathbf{z} and c , we also formulate a reconstruction loss \mathcal{L}_z on the latent variables \mathbf{z} , which control the content of an image. To this end, let \mathbf{e} denote the class unrelated content, extracted as $\mathbf{e} = E_e(G(\mathbf{z}, c))$, and define \mathcal{L}_z as:

$$\mathcal{L}_z = \mathbb{E}_{(\mathbf{z}, c) \sim p(\mathbf{z}, c)} \|\mathbf{z} - \mathbf{e}\|_2^2 \quad (5)$$

where E_e is the encoder responsible for extracting class unrelated content, and may share same layers with E_f . The smaller \mathcal{L}_z is, the better the content \mathbf{z} has been preserved.

In addition, in previous Eq. (3), we set the number of positive pairs, compared with negative pairs, is 1. This setting encourage each positive pair has large effect on calculating the contrastive loss, but not taking into account more positive pairs. Similarly, adding larger numbers of negatives to the denominator provides increased contrast for the positives. Following the work [19], we try to increase the number of positive pairs in contrastive loss formulation (*i.e.*, Eq. (3)) to weak this contrast, and may promote performance. Thus, for any (\mathbf{z}, c) , corresponding to \mathbf{f} , all positives, *i.e.*, all samples with the same c value, after sampling can be introduced to contribute the numerator, which may incur the relevant change of denominator.

Finally, the objective function for our CD-GAN takes account into the image reality (*i.e.*, \mathcal{L}_{GAN}), the contrastive loss (*i.e.*, \mathcal{L}_c) and the content consistency (*i.e.*, \mathcal{L}_z):

$$\mathcal{L}_G = \mathcal{L}_{GAN} + \beta_1 \mathcal{L}_c + \beta_2 \mathcal{L}_z \quad (6)$$

where β_1 and β_2 are two trade-off terms. To constrain the flexibility, we prefer to learn G and $E = \{E_f, E_e\}$ separately. After optimizing G , we optimize E . Finally, we update discriminator D according \mathcal{L}_D , which takes the same form as in our chosen GANs. The learning of CD-GAN is a two-step alternative optimization procedure: (i) update discriminator D , and (ii) update generator G and encoder $E = \{E_f, E_e\}$.

Algorithm 1 Minibatch stochastic optimization for CD-GAN.

Require: Initialize D, G , and E .

- 1: **for** number in training iterations **do**
 - 2: Generate minibatch of $2N$ examples: $\{\mathbf{x}_n^{fake}\}_{n=1}^{2N}$
 - 3: Sample minibatch of $2N$ examples: $\{\mathbf{x}_n^{real}\}_{n=1}^{2N}$
 - 4: Update D by ascending gradient: $\nabla_D \mathcal{L}_D$
 - 5: Sample minibatch of $2N$ noise samples: $\{(\mathbf{z}_n, c_n)\}_{n=1}^N$
 - 6: Update G by descending gradient with E fixed:

$$\nabla_G \{\mathcal{L}_{GAN} + \beta_1 \mathcal{L}_c + \beta_2 \mathcal{L}_z\}$$
 - 7: Update E by descending gradient with G fixed:

$$\nabla_E \{\beta_1 \mathcal{L}_c + \beta_2 \mathcal{L}_z\}$$
 - 8: **end for**
-

4. Using Few Labels

Our key idea is, in our contrastive disentanglement framework, to introduce some real examples with labels as anchor points and drag generated samples to be close to them. Compared with the unsupervised contrastive loss in Eq. (3), the main difference lies in the contrastive loss on positive pairs. For each sample generated from (\mathbf{z}, c) , the contrast on positive pairs becomes:

$$e^{(\mathbf{f}^T \mathbf{f}^+ / \tau)} + e^{(\mathbf{f}^T \mathbf{f}_{real}^+ / \tau)} \quad (7)$$

where $\mathbf{f} = E_f(G(\mathbf{z}, c))$, $\mathbf{f}^+ = E_f(G(\mathbf{z}^+, c^+))$, and \mathbf{f}_{real}^+ is extracted from a real image, which is sampled from a very small subset of real images with labels. Thus, for each generated image, we encourage its feature is close to one anchor point, which may make use of these few labels to the largest extent.

Similarly, the contrastive loss for negative pairs can take some examples from real images with different labels. Thus, the contrast here does not only means contrast with positive and negative pairs, but also means contrast fake examples with anchor points (*i.e.*, real images with few labels), which may largely promote the disentangling performance, even very few labels are involved.

5. Experiments

We evaluated the performance of our CD-GAN on a number of tasks and datasets to demonstrate its efficacy.

5.1. Benchmark Datasets

We use 5 benchmark datasets to evaluate our proposed CD-GAN, and the details of these datasets are described in the following: (i) MNIST [27]. It has 70,000 28×28 grayscale images of digits ranging from 0 to 9. The training set has 60000 samples. (ii) Fashion-MNIST [45]. It also has 70000 images with the size 28×28 . The 10 types of fashion products are: ankle boot, bag, coat, dress, pullover, sandal, shirt, sneaker, trouser and Tshirt. (iii) CIFAR-10 [24]. It has 60,000 labeled 32×32 RGB natural images in 10 classless. The 10 classes are: airplane, automobile, bird, cat, deer, dog, frog, horse, ship and truck. There are 50000 images for training. (iv) dSprites [32]. It consists of 737,280 binary 64×64 images of 2D shapes. It has 5 independent latent factors: shape, scale, rotation, x and y positions of a sprite. The shape contains three categories: square, ellipse and heart. (v) Faces [36]. It contains many latent factors as azimuth (pose), elevation, and lighting. We randomly generated 10,000 different faces and sampled 10 images at equal intervals from -90 degrees to 90 degrees for each face. Thus, the total number of images is 100000.

5.2. Experimental Setup

Evaluation Metrics. We used normalized clustering purity (ACC), normalized mutual information (NMI), and adjusted rank index (ARI) to evaluate our disentangling performance [34]. ACC is designed to calculate the percentage of correct clusters in total samples. NMI tend to evaluate cluster score by measuring the normalized mutual information between real labels and clustered labels. ARI is a metric that measures the similarity of the two clusters by evaluating the proportion of the correct clustering in all clustering results. Following the work [34], given test images, we adopted k -means to cluster the features encoded by E_f . Then, the above mentioned three metrics were used to evaluate performance. The reported the best ACC, NMI and ARI scores from 5 runs. In addition, to evaluate the generative performance, we use Inception Score (IS) [39] and Fréchet Inception Distance (FID) [16] for evaluation. The IS was calculated for 10 partitions of 50,000 randomly generated samples, and the FID was calculated for 50,000 samples.

Baselines. We compared our CD-GAN with the primary GANs based disentanglement methods, including: (i) GANs [11], (ii) InfoGAN [7], (iii) InfoGAN-CR [28], (iv) ClusterGAN [34]. We did not compare CD-GAN with VAE based disentanglement methods, as VAE based disentanglement has been well studied whereas GANs based disentanglement has been seldom explored. In fact, the generation performance of GANs should obviously better than VAE as VAE has a ℓ_2 reconstruction loss.

Implementation Details. The parameter settings, such as trade-offs, batch size, network architecture and optimization details are described in the following.

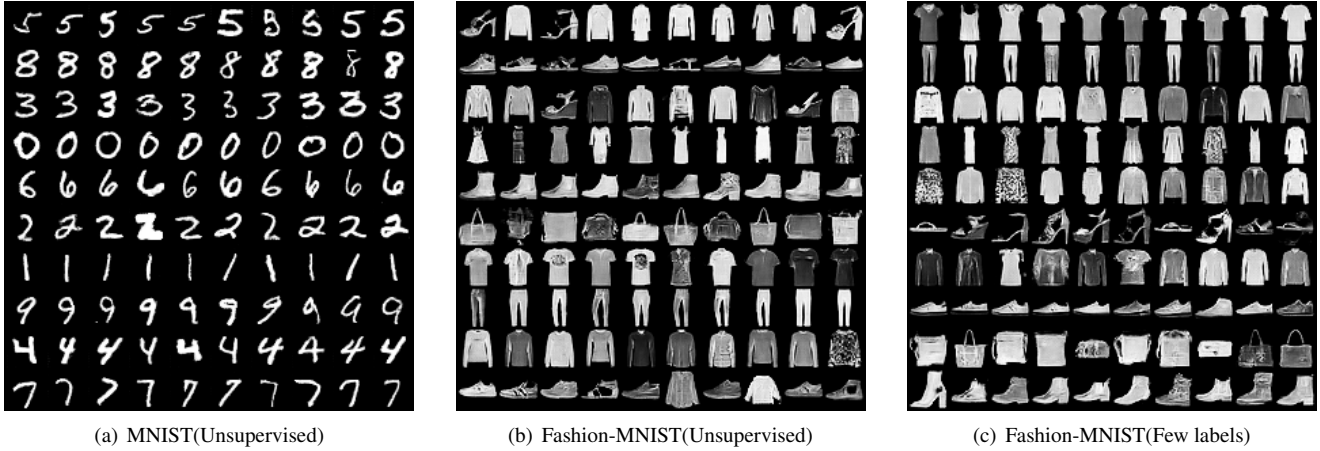


Figure 2. Images generated by CD-GAN trained on different datasets. Each row corresponds to one latent factor value. **(a):** Trained on MNIST with unsupervised setting. The images in each row have the same category. **(b):** Trained on Fashion-MNIST with unsupervised setting. The images in each row have the same category. **(c):** Trained on Fashion-MNIST with few labels. Obvious disentanglement performance can be found.

-MNIST. When calculating \mathcal{L}_c , the number of positives and negatives for each sample is the number of samples having the same factor value or having the different values. The network generator and discriminator architecture follows the work [34], which was WGAN-GP [12]. The encoder’s architecture is almost the same as the Discriminator. The batchsize for encoder, generator and discriminator were 512, 64, and 64. The dimension of \mathbf{z} was 30, and \mathbf{c} was one-hot with the dimension of 10. The dimension of the embedding \mathbf{f} and \mathbf{e} were set be 40 and 30, respectively. β_1 and β_2 were set to be 50 and 0.0005. The value of τ is set it be 0.07.

-FashionMNIST. The main parameters and experimental settings were set the same as the ones on the MNIST dataset. Some differences are list in the following. The batch size of encoder was set to be 1200, and the dimension of \mathbf{z} was set to be 40. The dimensions of \mathbf{f} and \mathbf{e} were 50 and 40 respectively, and $\beta_1 = 100$. In the experiment of introducing few labels, β_1 were set to be 50, and 2.4% of the training samples were with labels.

-CIFAR-10. The network architecture was set according to the work [33], which was SNGAN. The encoder’s architecture was ResNet18 [15]. The batch size of generator was 128, while it for discriminator and encoder were 64 and 256. The dimension of \mathbf{z} was 118, and the dimension of \mathbf{c} was 10. When calculating \mathcal{L}_c , the number of positives and negatives for each sample is the number of samples having the same factor value or having the different values. The dimension of \mathbf{f} and \mathbf{e} were 128 and 118 respectively. In addition, $\beta_1 = 1$, and $\beta_2 = 0.01$. The value of τ was 0.05. In the experiment of introducing few labels, 5% of the training samples were with labels, and β_2 were set to be 0.00005.

-dSprites. The shape variation was chosen as the target for disentanglement. The scale, rotation and translation changes

can be treated as intra-class variation. The network architecture follows the work [28], which was SNGAN. The encoder’s architecture follows the Q-network of the InfoGAN-CR [28] except the last layer. The batch size for was set to be 300 for generator and discriminator, and 1200 for encoder. 727,280 images were used for training and the rest 10,000 for testing. The dimension of \mathbf{z} was 52, and \mathbf{c} was one-hot with the dimension of 3. The dimension of \mathbf{f} and \mathbf{e} were 40 and 52, respectively. In addition, $\beta_1 = 1$, and $\beta_2 = 0.0001$. In the experiment, 1.2% of the training samples were set to have labels. The value of τ was 0.07.

-Faces. The network architecture for GANs were set according to the work [7], which was WGAN-GP. The encoder’s architecture was the same as the discriminator except the last layer. The batch size of generator and discriminator were 180, while the batch size of encoder was 3,600. The dimension of \mathbf{z} was 118, and the dimension of \mathbf{c} was 10. The dimension of the embedding \mathbf{f} and \mathbf{e} were 128 and 118, respectively. In addition, $\beta_1 = 10$, and $\beta_2 = 10$. 1% of the training samples were with labels. The value of τ was set to be 0.07.

5.3. Ablation Study

To test the validity of contrastive loss for disentangling inter-class variation, we set the value of β_1 to be zero. Then, the objective function only have two parts: (i) the GANs loss \mathcal{L}_{GAN} , and (ii) the content consistency loss \mathcal{L}_z . From the results in Fig. 2, we find there is no disentangling effect on both MNIST and Fashion-MNIST, even we also have a structured input, including content factor \mathbf{z} and class factor \mathbf{c} . Such results obviously demonstrate, through contrastive loss, we can disentangle the discrete variation of some factor.

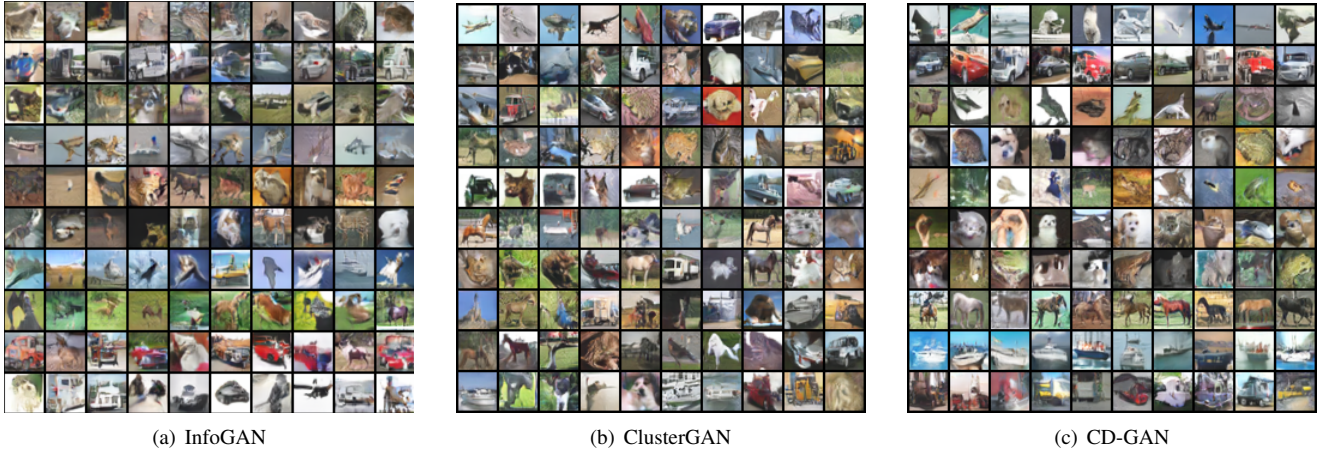


Figure 3. Images (with size 32×32) generated by different methods on CIFAR-10. Each row corresponds to one latent factor value. **(a):** InfoGAN. The images of each row have no obvious disentanglement results and the image quality is poor. **(b):** ClusterGAN. The images of each row have no obvious disentanglement results. **(c):** CD-GAN. Some obvious similar images can be found in one row, such as the 2nd, 8th and 9th rows.

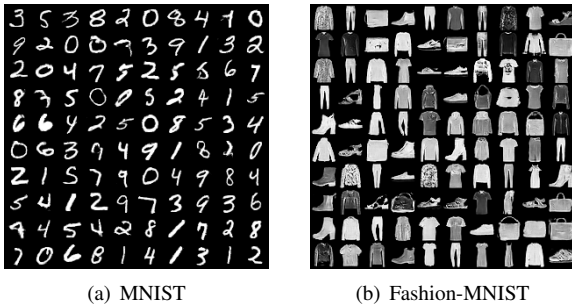


Figure 4. Images generated by CD-GAN without contrastive loss. Each row corresponds to one latent factor value, it is proved that disentanglement can not be resolved without contrast loss. **(a):** Trained on MNIST. **(b):** Trained on Fashion-MNIST.

5.4. Quantitative Results

Disentangled Results. Fig. 2 shows the disentangled results with training data on the MNIST, and Fashion-MNIST datasets. The images in each row are generated from fixed factor c and various noise z . The results on MNIST as in Fig 2 (a) show the generation results of our unsupervised CD-GAN, where different values of c controls digits from 0 to 9. In addition, this hints unsupervised disentanglement method may be capable of disentangling simple structured data. However, the results on Fashion-MNIST dataset changes to be worse as this dataset becomes more complex. From the work [34], we know unsupervised disentanglement methods fails to deal with this dataset to some extent. From Fig. 2 (c), we observe our CD-GAN with few labels can dramatically improves the disentanglement performance on the Fashion-MNIST dataset. This is due to the contrastive loss in CD-GAN, which can drag fake images to be close

to real ones in the same class, even the real ones are very limited.

Fig. 3 shows the disentanglement results of InfoGAN, ClusterGAN and CD-GAN on the CIFAR-10 dataset. From the results, we find InfoGAN and ClusterGAN both fail to disentangle the correct inter-class variation, since CIFAR-10 is much more complex than MNIST and FashionMNIST. Such results also demonstrate our claim that disentanglement learning should have limited amount of supervision. From Fig. 3, where 5% of training images have labels, we observe some inter-class variation can be disentangled. For example, the 2nd, 6th and 8th rows correspond to “automobile”, “dog”, “horse”.

Fig. 5 shows the disentangled results on dSprites dataset. Fig. 5 (a), (b) and (c) show the generation results of changing factor c and z , where the shape “square”, “ ellipse”, and “heart” are generated orderly. These results reveal our CD-GAN with few labels is robust to intra-class changes, such as scale, rotation and translation. This should own to the contrastive loss of our method, which not only contrasts the features associated with different factors, but also utilizes the few labels to the largest extent. The ACC, NMI and ARI scores are all close to 1, even only 1% of labels are involved.

Fig. 6 shows the disentangled results on Faces dataset, where each row corresponds to different head pose. We discretized the continuous pose change to discrete pose change, the angle gap between each class is 20° . We observe the images in adjacent categories are very similar, compared with digits, objects or shapes. The results show our CD-GAN has the capability to disentangle the inter-class variation, where the adjacent class are very similar. This further demonstrate the efficacy of our method for inter-class disentanglement.

t-SNE Results To further study how CD-GAN disentangle

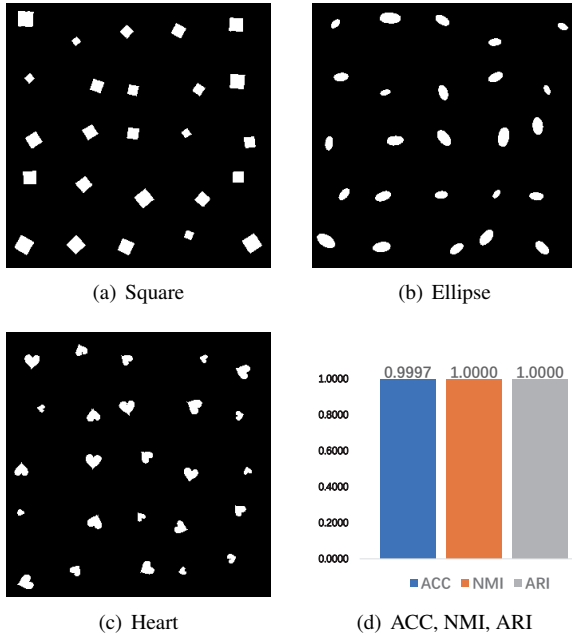


Figure 5. Images generated by CD-GAN on dSprites. (a), (b), and (c) represent the images corresponding to the three shapes, respectively. There is enough diversity in the images for each category. (d) is the result of the ACC, NMI and ARI score.

inter-class variation, we visualized the features \mathbf{f} , the output of E_f , by t-SNE on Fashion-MNIST dataset. We sampled 10000 points from $p(\mathbf{z}, c)$, and for each fixed c , the number of sampled points is the same. In Fig. 7, Different color corresponds to different values of factor c . We visualized the encoded features of unsupervised CD-GAN and CD-GAN with few labels.

Fig. 7 shows an obvious phenomenon, that is, CD-GAN with even approximate 2% labels have dramatically improved disentanglement result than unsupervised CD-GAN. This is due to our contrastive loss design, where each generated image are compared with one real images with labels. These real images with labels in CD-GAN disentanglement framework can be treated as anchor points, which may largely calibrate the generated images having the same class labels.

5.5. Qualitative Results

The results in Tabs. 1, Tab. 2 and Tab. 3 show some tendencies in the comparison with other baseline methods. (i) Our CD-GAN have achieve state-of-the-art performance, when compared with other baseline methods. The ACC, NMI and ARI score are 0.91, 0.93, and 0.94 on MNIST and 0.66, 0.62, 0.53 for unsupervised settings on Fashion-MNIST. As discussed in Sec. 3, the contrastive loss may have more powerful disentanglement capability, which not only considers the similarity of generated samples in one class,

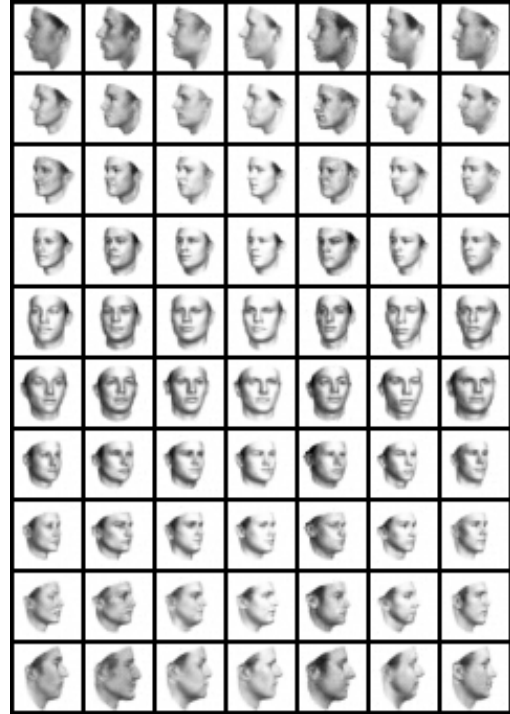


Figure 6. Images generated by CD-GAN trained on Faces. Each row corresponds to one latent factor value. Experiments show that the continuous variation of the same attribute can be controlled by adding loss \mathcal{L}_z .

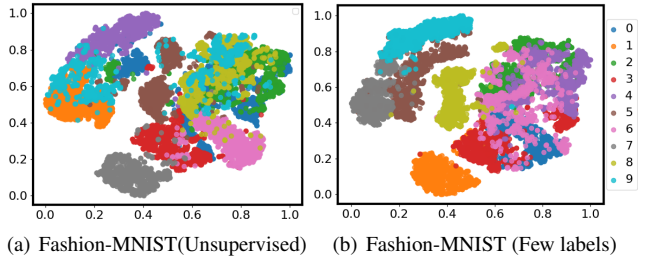


Figure 7. Visualization of the generated images by t-SNE on the Fashion-MNIST dataset. (a): Visualization of the generated images by CD-GAN with unsupervised training. (b): Visualization of the generated images by CD-GAN with limited amount of supervision. It shows that limited amount of supervision guides better disentanglement.

but also utilizes the dissimilarity of samples in different class. (ii) Our CD-GAN with few labels (usually 1-2%) can dramatically promote the disentanglement performance. As we discussed previously, this is due to the contrastive loss in CD-GAN, which provide us a way to have real images with labels as anchor points and calibrate generated images by virtue of them. (iii) On especially complex dataset, such as CIFAR-10, all unsupervised methods fails, where the ACC is close to 0.1. Our CD-GAN with few labels (with 5%) can have much better performance than ClusterGAN, which

Algorithm	ACC	NMI	ARI
ClusterGAN [34]	0.95	0.89	0.89
Info-GAN [7]	0.89	0.86	0.82
Info-GAN-CR [28]	0.90*	0.91*	0.92*
GAN with bp [34]	0.95	0.90	0.89
GAN with Disc. ϕ [34]	0.70	0.62	0.52
CD-GAN (Unsupervised)	0.91	0.93	0.94

Table 1. Comparison of disentanglement Result on MNIST. * denotes the results obtained by ours running.

Algorithm	ACC	NMI	ARI
ClusterGAN [34]	0.63	0.64	0.50
Info-GAN [7]	0.61	0.59	0.44
Info-GAN-CR [28]	0.61*	0.52*	0.41*
GAN with bp [34]	0.56	0.53	0.37
GAN with Disc. ϕ [34]	0.43	0.37	0.23
CD-GAN (Unsupervised)	0.66	0.62	0.53
CD-GAN (Few labels)	0.82	0.72	0.68

Table 2. Comparison of disentanglement Result on Fashion-MNIST. * denotes the results obtained by ours running.

Algorithm	ACC	IS	FID
ClusterGAN [34]	0.14*	7.26*	26.86*
Info-GAN [7]	-	7.19*	28.20*
Info-GAN-CR [28]	-	6.81*	29.82*
CD-GAN (Few labels)	0.41	7.65	23.97

Table 3. Comparison of disentanglement Result and evaluating Inception Score(IS) and Frechet Inception Distance(FID) on CIFAR-10. * denotes the results obtained by ours running.

dramatically promote the disentanglement performance afforded by unsupervised methods. This is also due to the contrastive disentanglement strategy.

Tab. 3 also shows the FID comparison between CD-GAN, InfoGAN, InfoGAN-CR and ClusterGAN on CIFAR-10 dataset, where each method adopts SNGAN architecture. This result shows our IS and FID for unsupervised setting are 7.38 and 25.40 while ClusterGAN’s IS and FID are 7.26 and 26.86. Obviously, such results are much better than InfoGAN and InfoGAN-CR, in which the mutual information regularization may limit diversity. Moreover, by virtue of few labels, our CD-GAN further improved IS and FID.

6. Conclusion and Future Work

Contrastive loss was introduced in generative adversarial networks to construct a contrastive disentanglement framework for interpretable representation learning. By virtue of contrastive loss, we formulated the correlation between the disentangled factor values and inter-class image variation.

Moreover, we analyzed the advantage of formulating contrastive loss for preventing mode collapse in GAN’s training. We provided a new way to make use of limited amount of supervision to the largest extent in disentangling complex data. We demonstrated the efficacy of our CD-GAN on many well-known tasks and public datasets.

In the current work, we use a moderate batchsize in parameter learning, which may limit the capability of contrastive learning. Although our results indicate such a choice is effective, it is worth to explore extremely large batchsize for performance promotion further. In addition to apply contrastive learning for inter class variation disentanglement, we are currently investigating the possibility of applying it for more complex factor disentangling problem.

References

- [1] Maruan Al-Shedivat, Avinava Dubey, and Eric P. Xing. Contextual explanation networks. *Journal of Machine Learning Research*, 21(194):1–44, 2017. 1
- [2] Martin Arjovsky, Soumith Chintala, and Léon Bottou. Wasserstein GAN. In *ICML*, pages 214–223, 2015. 1
- [3] David Barber and Felix Agakov. The im algorithm: a variational approach to information maximization. In *NIPS*, pages 201–208, 2003. 1
- [4] David Bau, Jun-Yan Zhu, Hendrik Strobelt, Bolei Zhou, Joshua B. Tenenbaum, William T. Freeman, and Antonio Torralba. Gan dissection: Visualizing and understanding generative adversarial networks. In *ICLR*, 2018. 1
- [5] Ting Chen, Simon Kornblith, Mohammad Norouzi, and Geoffrey Hinton. A simple framework for contrastive learning of visual representations. 2020. 1, 2
- [6] Tian Qi Chen, Xuechen Li, Roger B. Grosse, and David Duvenaud. Isolating sources of disentanglement in variational autoencoders. In *ICLR*, 2018. 2
- [7] Xi Chen, Yan Duan, Rein Houthoofd, John Schulman, Ilya Sutskever, and Pieter Abbeel. Infogan: interpretable representation learning by information maximizing generative adversarial nets. In *NIPS*, pages 2180–2188, 2016. 1, 2, 4, 5, 8
- [8] Finale Doshi-Velez and Been Kim. Towards a rigorous science of interpretable machine learning. *arXiv preprint arXiv:1702.08608*, 2017. 1
- [9] Patrick Esser, Robin Rombach, and Bjorn Ommer. A disentangling invertible interpretation network for explaining latent representations. In *CVPR*, pages 9223–9232, 2020. 2
- [10] Aviv Gabbay and Yedid Hoshen. Demystifying inter-class disentanglement. In *ICLR*, 2020. 1
- [11] Ian Goodfellow, Jean Pouget-Abadie, Mehdi Mirza, Bing Xu, David Warde-Farley, Sherjil Ozair, Aaron Courville, and Yoshua Bengio. Generative adversarial nets. In *NIPS*, pages 2672–2680, 2014. 1, 4
- [12] Ishaan Gulrajani, Faruk Ahmed, Martin Arjovsky, Vincent Dumoulin, and Aaron C Courville. Improved training of Wasserstein GANs. In *NIPS*, pages 5767–5777, 2017. 1, 5
- [13] Michael Gutmann and Aapo Hyvärinen. Noise-contrastive estimation: A new estimation principle for unnormalized

- statistical models. *Journal of Machine Learning Research*, 9:297–304, 2010. 2
- [14] Kaiming He, Haoqi Fan, Yuxin Wu, Saining Xie, and Ross Girshick. Momentum contrast for unsupervised visual representation learning. 2019. 1, 2
- [15] Kaiming He, Xiangyu Zhang, Shaoqing Ren, and Jian Sun. Deep residual learning for image recognition. In *2016 IEEE Conference on Computer Vision and Pattern Recognition (CVPR)*, pages 770–778, 2016. 5
- [16] Martin Heusel, Hubert Ramsauer, Thomas Unterthiner, Bernhard Nessler, and Sepp Hochreiter. Gans trained by a two time-scale update rule converge to a local nash equilibrium. In *NIPS*, pages 6626–6637, 2017. 4
- [17] Irina Higgins, Loic Matthey, Arka Pal, Christopher Burgess, Xavier Glorot, Matthew Botvinick, Shakir Mohamed, and Alexander Lerchner. beta-vae: Learning basic visual concepts with a constrained variational framework. In *ICLR*, 2016. 1, 2
- [18] Insu Jeon, Wonkwang Lee, and Gunhee Kim. Ib-gan: Disentangled representation learning with information bottleneck gan. 2018. 1
- [19] Prannay Khosla, Piotr Teterwak, Chen Wang, Aaron Sarna, Yonglong Tian, Phillip Isola, Aaron Maschiot, Ce Liu, and Dilip Krishnan. Supervised contrastive learning. 2020. 1, 2, 3
- [20] Hyunjik Kim and Andriy Mnih. Disentangling by factorising. In *ICML*, pages 2649–2658, 2018. 1, 2
- [21] Diederik P Kingma, Shakir Mohamed, Danilo Jimenez Rezende, and Max Welling. Semi-supervised learning with deep generative models. In *NIPS*, volume 27, pages 3581–3589, 2014. 1
- [22] Diederik P Kingma and Max Welling. Auto-encoding variational bayes. In *ICLR*, 2014. 1
- [23] Murat Kocaoglu, Christopher Snyder, Alexandros G. Dimakis, and Sriram Vishwanath. Causalgan: Learning causal implicit generative models with adversarial training. In *ICLR*, 2018. 1
- [24] A. Krizhevsky. Learning multiple layers of features from tiny images. 2009. 1, 4
- [25] Tejas D. Kulkarni, William F. Whitney, Pushmeet Kohli, and Joshua B. Tenenbaum. Deep convolutional inverse graphics network. In *NIPS*, volume 28, pages 2539–2547, 2015. 1
- [26] Himabindu Lakkaraju, Stephen H. Bach, and Jure Leskovec. Interpretable decision sets: A joint framework for description and prediction. In *Proceedings of the 22nd ACM SIGKDD International Conference on Knowledge Discovery and Data Mining*, volume 2016, pages 1675–1684, 2016. 1
- [27] Yann Lecun, Leon Bottou, Yoshua Bengio, and Patrick Haffner. Gradient-based learning applied to document recognition. *Intelligent Signal Processing*, pages 306–351, 2001. 1, 4
- [28] Zinan Lin, Kiran Thekumparampil, Giulia Fanti, and Sewoong Oh. Infogan-cr: Disentangling generative adversarial networks with contrastive regularizers. In *ICML*, volume 1, 2020. 2, 4, 5, 8
- [29] Bingchen Liu, Yizhe Zhu, Zuohui Fu, Gerard de Melo, and Ahmed Elgammal. Oogan: Disentangling gan with one-hot sampling and orthogonal regularization. In *AAAI*, volume 34, pages 4836–4843, 2020. 1
- [30] Francesco Locatello, Stefan Bauer, Mario Lucic, Gunnar Ratsch, Sylvain Gelly, Bernhard Scholkopf, and Olivier Bachem. Challenging common assumptions in the unsupervised learning of disentangled representations. In *ICLR*, 2019. 1, 2
- [31] Francesco Locatello, Michael Tschannen, Stefan Bauer, Gunnar Ratsch, Bernhard Scholkopf, and Olivier Bachem. Disentangling factors of variations using few labels. In *ICLR*, 2020. 1, 2
- [32] Loic Matthey, Irina Higgins, Demis Hassabis, and Alexander Lerchner. dsprites: Disentanglement testing sprites dataset. <https://github.com/deepmind/dsprites-dataset/>, 2017. 1, 4
- [33] Takeru Miyato, Toshiki Kataoka, Masanori Koyama, and Yuichi Yoshida. Spectral normalization for generative adversarial networks. *arXiv preprint arXiv:1802.05957*, 2018. 1, 5
- [34] Sudipto Mukherjee, Himanshu Asnani, Eugene Lin, and Sreeram Kannan. Clustergan: Latent space clustering in generative adversarial networks. In *AAAI*, volume 33, pages 4610–4617, 2019. 2, 3, 4, 5, 6, 8
- [35] Sebastian Nowozin, Botond Cseke, and Ryota Tomioka. f-GAN: Training generative neural samplers using variational divergence minimization. In *NIPS*, pages 271–279, 2016. 1
- [36] P. Paysan, R. Knothe, B. Amberg, S. Romdhani, and T. Vetter. A 3d face model for pose and illumination invariant face recognition. In *2009 Sixth IEEE International Conference on Advanced Video and Signal Based Surveillance*, pages 296–301, 2009. 1, 4
- [37] Alec Radford, Luke Metz, and Soumith Chintala. Unsupervised representation learning with deep convolutional generative adversarial networks. In *ICLR*, 2016. 1
- [38] Cynthia Rudin. Stop explaining black box machine learning models for high stakes decisions and use interpretable models instead. *Nature Machine Intelligence*, 1(5):206–215, 2019. 1
- [39] Tim Salimans, Ian Goodfellow, Wojciech Zaremba, Vicki Cheung, Alec Radford, and Xi Chen. Improved techniques for training GANs. In *NIPS*, pages 2234–2242, 2016. 1, 4
- [40] Yujun Shen, Jinjin Gu, Xiaoou Tang, and Bolei Zhou. Interpreting the latent space of gans for semantic face editing. In *CVPR*, pages 9243–9252, 2020. 2
- [41] Rui Shu, Yining Chen, Abhishek Kumar, Stefano Ermon, and Ben Poole. Weakly supervised disentanglement with guarantees. In *ICLR*, 2020. 1
- [42] Kihyuk Sohn. Improved deep metric learning with multi-class n-pair loss objective. In *NIPS*, pages 1857–1865, 2016. 1, 2
- [43] Kihyuk Sohn, Xinchun Yan, and Honglak Lee. Learning structured output representation using deep conditional generative models. In *NIPS*, pages 3483–3491, 2015. 1
- [44] Zhirong Wu, Yuanjun Xiong, Stella X Yu, and Dahua Lin. Unsupervised feature learning via non-parametric instance discrimination. In *CVPR*, pages 3733–3742, 2018. 1, 2
- [45] Han Xiao, Kashif Rasul, and Roland Vollgraf. Fashion-mnist: a novel image dataset for benchmarking machine learning algorithms, 2017. 1, 4
- [46] Quanshi Zhang, Ruiming Cao, Feng Shi, Ying Nian Wu, and Song-Chun Zhu. Interpreting cnn knowledge via an explanatory graph. In *AAAI*, pages 4454–4463, 2017. 1

- [47] Quanshi Zhang, Ying Nian Wu, and Song-Chun Zhu. Interpretable convolutional neural networks. In *CVPR*, pages 8827–8836, 2018. [1](#)
- [48] Quanshi Zhang, Yu Yang, Haotian Ma, and Ying Nian Wu. Interpreting cnns via decision trees. In *CVPR*, pages 6261–6270, 2019. [1](#)